

Transverse energy and forward energy production in a high energy nuclear collision model

Jing-Ye Zhang, Xiaochun He, and Chia C. Shih
University of Tennessee, Knoxville, Tennessee 37796

Soren P. Sorensen
University of Tennessee, Knoxville, Tennessee 37796
and Oak Ridge National Laboratory, Oak Ridge, Tennessee 37831

Cheuk-Yin Wong
Oak Ridge National Laboratory, Oak Ridge, Tennessee 37831
(Received 7 April 1992)

Distributions of transverse energy, forward energy, and $dE_T/d\eta$ from 60A GeV and 200A GeV ^{16}O -induced and 200A GeV ^{32}S -induced nuclear collision with Al, Cu, Ag, and Au are calculated by a high energy nuclear collision model and compared to recent experimental data from the WA80 Collaboration at CERN. The high energy nuclear collision Monte Carlo model, which is based on the concept of independent multiple nucleon-nucleon collisions, describes the experimental data at forward-rapidity and midrapidity well.

PACS number(s): 25.75.+r

I. INTRODUCTION

The heavy ion programs at the Brookhaven Alternating Gradient Synchrotron and CERN Super Proton Synchrotron accelerators have within the last five years provided a wealth of experimental data on high energy nuclear collisions. The aim of the experimental programs has been both the detection of the quark-gluon plasma (QGP) and a better understanding of the reaction mechanisms [1, 2]. In this paper the focus will be placed on the latter and we will discuss global variables like the transverse energy and the pseudorapidity distribution of the transverse energy, which have proved to be especially valuable for obtaining information on the reaction mechanisms. The framework for the discussion will be a comparison between, on one hand, the theoretical results obtained by the high energy nuclear collision Monte Carlo model MARCO [3] and, on the other hand, the experimental results from WA80 on calorimeter measured global variables [4]. We will especially focus on a discussion of the systematics of the $dE_T/d\eta$ distributions as function of impact parameter, projectile and target mass, and bombarding energy.

Section II contains a description of the key ingredients in the MARCO model. Section III discusses comparisons between the MARCO results and the WA80 data for forward energy, transverse energy, and $dE_T/d\eta$. In Sec. IV the strengths and shortcomings of MARCO are discussed and finally Sec. V contains the conclusions.

II. MARCO

A detailed description of the high energy nuclear collision Monte Carlo model MARCO is given in Ref. [3]. The basic assumptions in the model are the following: (a) A

high energy nucleus-nucleus collision can be considered as a superposition of individual nucleon-nucleon collisions. (b) The positions of the nucleons within each nucleus are chosen according to Gaussian density distributions for lighter nuclei and Woods-Saxon density distributions for heavier nuclei. (c) Only binary collisions consisting of a projectile and a target nucleon are considered (no rescattering). (d) The number of collisions a particular nucleon will encounter is calculated assuming an interaction cross section of 29.4 mb and straight-line trajectories. (e) The longitudinal momentum loss of each of the colliding nucleons in their mutual center-of-mass frame is given by the following stopping law for the light-cone variable x originally proposed by Kinoshita, Minaka, and Sumiyoshi [5] ($x_L < x < 1$):

$$P(x) = \frac{\alpha}{1-x_L} \left(\frac{x-x_L}{1-x_L} \right)^{\alpha-1},$$

$$x = \frac{E' + p'_z}{E + p_z},$$

$$x_L = \frac{m}{(E + p_z)_{\text{lab}}},$$

where (E, p_z) and (E', p'_z) are the energy and the longitudinal momentum of the nucleon before and after the collision, respectively. The stopping power parameter α is close to unity for free nucleon-nucleon collisions and in Ref. [3] $\alpha \simeq 1$ was also found to give a good description of ^{16}O +nucleus data. (f) The longitudinal energy loss is used for production of pions with the following rapidity and transverse momentum distribution:

$$P(y, p_T) \propto [(x_+^{\text{max}} - x_+) (x_-^{\text{max}} - x_-)]^{\alpha-1} f_\pi(p_T),$$

$$f_\pi(p_T) = \begin{cases} p_T \exp(-5.5p_T) & \text{if } p_T \leq 0.9 \text{ GeV}/c, \\ 0.532p_T \exp(-4.8p_T) & \text{if } p_T > 0.9 \text{ GeV}/c, \end{cases}$$

with p_T in units of GeV. x_{\pm} are the forward and backward light-cone variables, respectively, and x_{\pm}^{\max} are their corresponding maximum values after the light-cone momentum fractions of the leading baryons have been subtracted. Based on comparisons to nucleon-nucleon data the exponent a can be parametrized as $a = 3.5 + 0.7 \ln \sqrt{s}$.

The only difference in formulation between the model described in Ref. [3] and the current version is the inclusion of kaon production [with a transverse momentum distribution given by $\exp(-3.6/p_T)$]. The resulting transverse and forward energies are only slightly affected by this modification, which only seems to have a significant effect on the ratio between electromagnetic and hadronic energy as discussed in Sec. III.

The main virtue of MARCO is its simplicity. It represents the simplest possible generalization of a heavy ion collision in terms of nucleon-nucleon collisions. In this paper all model parameters, like α , a , etc., will be kept fixed at values determined from experimental data on free nucleon-nucleon collisions.

The purpose of this paper is to investigate how well the global features of ultrarelativistic nucleus-nucleus collisions can be understood by this simple model without the need to incorporate more complicated assumptions.

III. COMPARISON TO WA80 CALORIMETER DATA

We have chosen to compare the results of MARCO to the extensive set of calorimeter data recently published by the WA80 Collaboration [4]. The data set contains results from 60A GeV and 200A GeV ^{16}O -induced reactions and 200A GeV ^{32}S -induced reactions on targets of C, Al, Cu, Ag, and Au. The procedures described in Ref. [4] for simulating the effects of the trigger conditions and for obtaining the impact parameter dependence have been closely followed. The energy deposited in a calorimeter has been assumed to be the kinetic energy for nucleons and the total relativistic energy for pions and kaons.

A. Forward energy distributions

The forward energy E_f is defined as the sum of the energy carried by all particles with pseudorapidity $\eta > 6.0$. The forward energy distributions $d\sigma/dE_f$ shown in Fig. 1 depend at large values of E_f critically on the collision geometry, whereas the strength of the ‘‘bump’’ observed at low value of E_f for the Au-target reactions depends on the magnitude of the nuclear stopping power.

Qualitatively MARCO reproduces most of the features observed in the experimental E_f spectra, but quantitatively there are several differences. MARCO predicts the correct positions, but underestimates the strength by $\approx 30\%$, of the low energy ‘‘bump’’ in the Au spectra. This could indicate that the nuclear stopping parameter α should have a lower value than unity; but in Ref. [3] it was shown that other values of α lead to worse fits for the transverse energy.

MARCO reproduces the triangular shape of the approximately equal mass collisions O+C and S+Al, but seems to underestimate the total cross sections. This effect might be caused by projectile spectator breakup, which is ignored in MARCO. If this breakup produces one or several fragments with sufficiently large transverse momentum, so their pseudorapidity is shifted below 6.0, these fragments will not be absorbed by the forward calorimeter. This will imply a complicated downward shift of the E_f spectra and will lead to larger minimum bias cross sections. The breakup effect is expected to be strongest at the lowest beam energy, where the ratio between the transverse and longitudinal momenta will be largest, which is consistent with the observation, that the largest discrepancy between the experimental data and MARCO is found for 60A GeV $^{16}\text{O}+^{12}\text{C}$.

B. Transverse energy distributions

The transverse energy distributions shown in Fig. 2 have been obtained in the interval $2.4 < \eta < 5.5$. Again

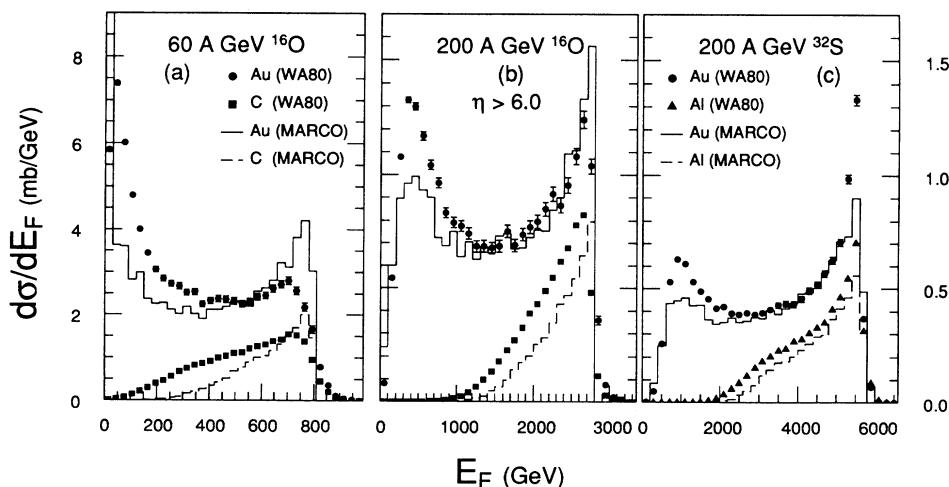


FIG. 1. Forward energy distributions ($\eta > 6.0$) for the following projectiles: (a) 60A GeV ^{16}O , (b) 200A GeV ^{16}O , and (c) 200A GeV ^{32}S . For ^{16}O -induced collisions the targets shown are ^{197}Au and ^{12}C and for ^{32}S -induced collisions the targets are ^{197}Au and ^{27}Al . In this and all following figures in this paper the experimental WA80 results are shown as symbols and the MARCO calculations are shown as histograms.

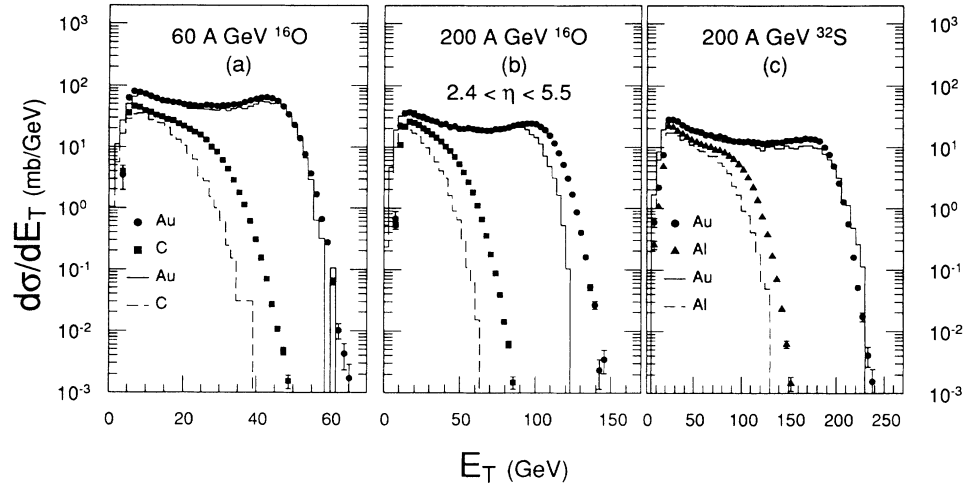


FIG. 2. Transverse energy distributions ($2.4 < \eta < 5.5$) for the same systems illustrated in Fig. 1.

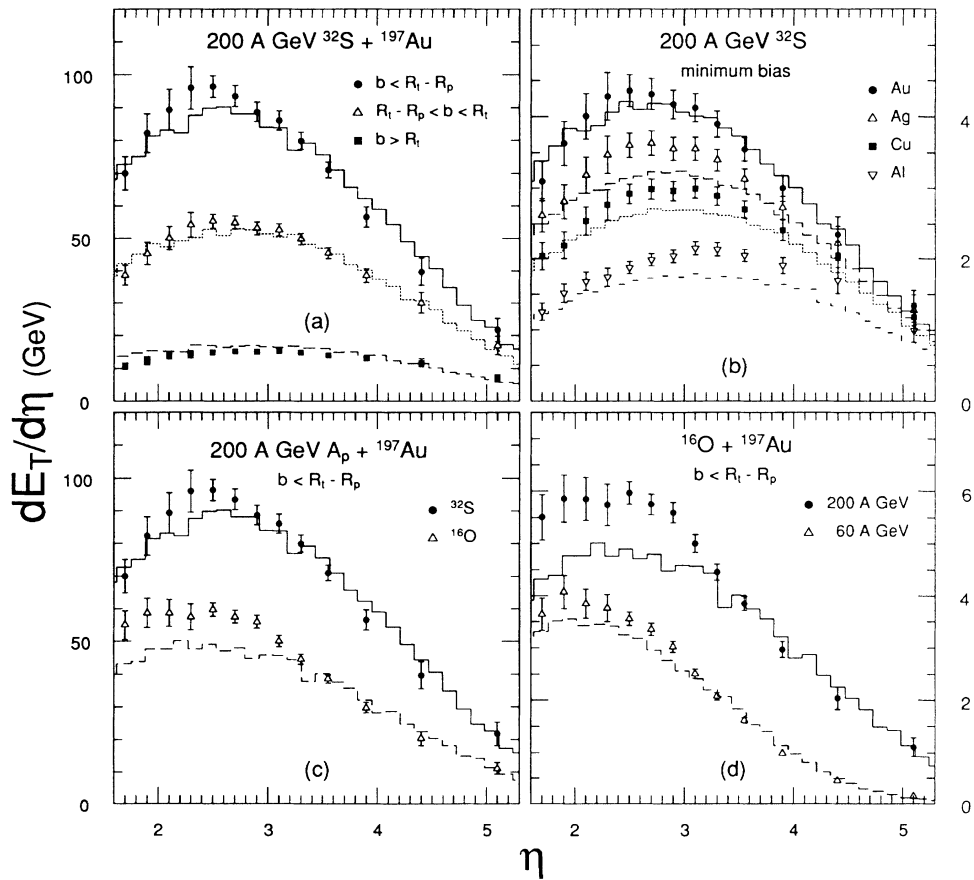


FIG. 3. A comparison between $dE_T/d\eta$ distributions from MARCO (histograms) and WA80 (symbols): (a) Impact parameter dependence for 200A GeV $^{32}\text{S}+^{197}\text{Au}$ (refer to Ref. [4] for a discussion on the method for obtaining the impact parameter cuts). (b) Target dependence for 200A GeV ^{32}S impinging on Al, Cu, Ag, and Au, respectively (minimum bias trigger conditions). (c) Projectile dependence for central collisions of 200A GeV ^{16}O and ^{32}S impinging on Au. (d) Beam energy dependence for central collisions of 60A GeV and 200A GeV $^{16}\text{O}+^{197}\text{Au}$.

MARCO qualitatively provides a good description of the experimental data. In general the fits are best for the heavy target ^{197}Au , whereas the calculated transverse energies for the light targets ^{12}C and ^{27}Al are too small. It is interesting to note that for central events in 60A GeV $^{16}\text{O}+^{197}\text{Au}$ and 200A GeV $^{32}\text{S}+^{197}\text{Au}$, where MARCO does not fit the E_f spectra very well, it nevertheless provides a perfect fit to the E_T spectra. We do not consider the discrepancy of $\approx 10\%$ between MARCO and the data for central events at 200A GeV $^{16}\text{O}+^{197}\text{Au}$ significant in view of the 10% systematic uncertainty quoted by WA80 [4] on the overall E_T energy scale.

As was the case for the E_f spectra also the E_T spectra show the worst disagreement for the lighter targets. The breakup effect described in the preceding section could qualitatively provide at least part of the explanation for the discrepancy, but only a much more complicated simulation with full rescattering incorporated will be able to provide a quantitative answer.

C. $dE_T/d\eta$ distributions

The $dE_T/d\eta$ distributions shown in the Figs. 3 and 4 can add considerably to our understanding of the reaction mechanisms. Before discussing these distributions in more detail it is, however, prudent to insert a word of

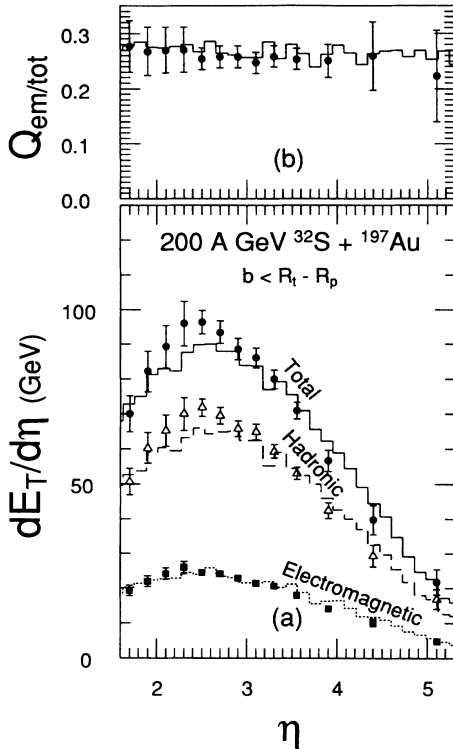


FIG. 4. (a) Comparison between $dE_T/d\eta$ distributions from MARCO (histograms) and WA80 (symbols) concerning the partition between electromagnetic, hadronic, and total transverse energy for central collisions of 200A GeV $^{32}\text{S}+^{197}\text{Au}$. (b) Ratio between the electromagnetic and total part of the $dE_T/d\eta$ distribution.

caution: the overall magnitude of $dE_T/d\eta$ distributions is in general very sensitive to the trigger and gating conditions used in their construction, and small uncertainties in the implementation of the minimum bias trigger conditions can severely affect the quality of the fits between the experimental data and the simulation results.

It is instructive from the outset to describe qualitatively the expectations for the $dE_T/d\eta$ distributions from a microscopic model like MARCO. The rapidity distribution of the pions produced from each binary inelastic nucleon-nucleon collision will be centered around the initial nucleon-nucleon center-of-mass rapidity and will extend slightly beyond the initial nucleon rapidities. As the nucleons suffer additional collisions their rapidities will decrease, so the nucleons experiencing the largest number of collisions will on the average have the largest rapidity losses. As a consequence, in an asymmetric nuclear collision, the nucleons from the smaller nucleus will on the average experience a larger rapidity change than nucleons from the larger nucleus. We can therefore expect that as we increase the target mass the average “effective midrapidity” of the pions will slowly move from the initial nucleon-nucleon midrapidity towards the target rapidity.

As a nucleon is experiencing more and more collisions the pions produced in these collisions will be more and more concentrated around the “effective midrapidity.” As a consequence, we will expect the pseudorapidity distributions to be more and more focused as the impact parameter decreases. In the following we will investigate if these simple consequences of the MARCO picture are reflected in the data.

All experimental and MARCO $dE_T/d\eta$ distributions have been fitted with Gaussian distributions in order to extract three parameters: the maximum value $dE_T/d\eta|_{max}$, the centroid (η), and the standard deviation σ_η . The systematic behavior of these three parameters as functions of centrality, beam energy, projectile, and target is shown in Tables I–III.

Figures 3(a)–3(d) demonstrate the impact parameter, target, projectile, and beam energy dependence of the $dE_T/d\eta$ distributions. Considering the simplicity of MARCO the overall agreement between the data and MARCO is very good, but some systematic deviations are noticeable: MARCO’s values for $dE_T/d\eta|_{max}$ are typically $\approx 10\%$ smaller than the experimental values and the calculated η centroids are slightly larger. The calculated and measured widths show a remarkable agreement.

The reason for large deviations found in 200A GeV $^{16}\text{O}+^{197}\text{Au}$ is not well understood. The ^{16}O data were obtained during a single running period, whereas the ^{32}S data were obtained at a later date. A systematic deviation between how well MARCO would fit the ^{16}O and the ^{32}S data might be explained by differences in the experimental calibration of the calorimeters. Calibration differences, however, cannot explain why MARCO generally fits the 60 GeV data ^{16}O data better than the 200 GeV data, since these data were recorded during the same run period with constant settings of the calorimeter.

As was observed for the transverse energy distributions the agreement for $dE_T/d\eta|_{max}$ is best for the heavy

TABLE I. The maximum value $dE_T/d\eta|_{\max}$ obtained from performing Gaussian fits to both the MARCO and the WA80 $dE_T/d\eta$ distributions.

Target	$dE_T/d\eta$ (max) GeV					
	60A ^{16}O		200A ^{16}O		200A ^{32}S	
	exp	theo	exp	theo	exp	theo
Central						
Cu	29.2	27.0	42.2	35.0	69.4	61.9
Ag	33.4	31.1	49.8	40.3	81.9	74.4
Au	39.5	35.0	60.2	48.9	92.9	89.1
Intermediate						
C	11.9	8.9	16.2	11.5		
Al					32.2	24.9
Cu	19.7	16.6	23.7	21.4	47.1	39.3
Ag	21.0	19.8	30.0	23.0	55.0	44.3
Au	22.9	20.9	33.6	27.0	54.1	53.0
Peripheral						
C	5.7	4.8	8.3	5.7		
Al					13.7	11.9
Cu	7.3	6.3	9.6	7.3	17.5	14.9
Ag	7.3	7.1	11.1	7.5	18.8	15.8
Au	7.4	7.3	11.2	9.2	15.3	17.2

targets and becomes gradually worse for lighter targets. MARCO has been carefully designed to fit a large range of proton-proton scattering data, so the large deviation for the lightest nuclear system is a puzzle.

It is remarkable how well MARCO reproduces the partition between “electromagnetic” and hadronic transverse energy as demonstrated in Fig. 4. MARCO assumes that $\frac{1}{3}$ of all created pions are π^0 's, which primarily will decay to photons. MARCO has no particle decay built in, so the electromagnetic transverse energy has been calculated based on the π^0 momenta.

TABLE II. The centroid value $\langle\eta\rangle$ obtained from performing Gaussian fits to both the MARCO and the WA80 $dE_T/d\eta$ distributions.

Target	$\langle\eta\rangle$					
	60A ^{16}O		200A ^{16}O		200A ^{32}S	
	exp	theo	exp	theo	exp	theo
Central						
Cu	2.34	2.39	2.62	2.89	2.89	3.00
Ag	2.19	2.25	2.44	2.75	2.67	2.86
Au	2.00	2.18	2.19	2.54	2.56	2.69
Intermediate						
C	2.81	2.70	3.09	3.28		
Al					3.23	3.17
Cu	2.40	2.43	2.73	2.94	2.92	3.00
Ag	2.30	2.35	2.57	2.88	2.78	2.93
Au	2.16	2.26	2.41	2.73	2.73	2.79
Peripheral						
C	2.68	2.56	2.97	3.19		
Al					3.24	3.13
Cu	2.51	2.43	2.78	2.98	3.01	3.01
Ag	2.46	2.42	2.71	2.99	2.94	2.93
Au	2.38	2.36	2.67	2.87	2.97	2.87

TABLE III. The standard deviation σ_η obtained from performing Gaussian fits to both the MARCO and the WA80 $dE_T/d\eta$ distributions.

Target	σ_η					
	60A ^{16}O		200A ^{16}O		200A ^{32}S	
	exp	theo	exp	theo	exp	theo
Central						
Cu	1.14	1.19	1.43	1.56	1.41	1.54
Ag	1.15	1.20	1.44	1.53	1.44	1.52
Au	1.16	1.18	1.47	1.51	1.39	1.46
Intermediate						
C	1.24	1.28	1.47	1.63		
Al					1.50	1.58
Cu	1.23	1.24	1.50	1.56	1.48	1.53
Ag	1.24	1.22	1.50	1.56	1.49	1.53
Au	1.26	1.24	1.55	1.55	1.46	1.51
Peripheral						
C	1.34	1.35	1.60	1.64		
Al					1.64	1.61
Cu	1.35	1.32	1.63	1.63	1.63	1.60
Ag	1.37	1.30	1.62	1.64	1.65	1.64
Au	1.39	1.31	1.62	1.65	1.69	1.63

IV. DISCUSSION

It is remarkable that a model as simple and transparent as MARCO can obtain the degree of agreement with the experimental data as demonstrated in the preceding section. To us this demonstrates that the global features of high energy nuclear collisions to first order can be described as a superposition of free nucleon-nucleon collisions with collision probabilities depending on the nuclear geometry.

In order to obtain an even closer agreement with the data in the midrapidity region the most likely improvement of the model might be the incorporation of rescattering effects between spectator and participant nucleons, pions and nucleons, and pions and pions. Monte Carlo models like VENUS [6], MCFM [7], and HIJET [8], which have included rescattering in a variety of different ways, have demonstrated the importance of rescattering effects. For an asymmetric projectile-target combination ($A_p < A_t$) rescattering tends to move the η centroid to smaller values and at the same time increase the transverse energy. Since MARCO in general underestimates $dE_T/d\eta|_{\max}$ and slightly overestimated the η centroid inclusion of rescattering, one could probably qualitatively improve MARCO's agreement with the data. How well the quantitative agreement would be is, however, very difficult to estimate, since the various codes incorporating rescattering obtain different estimates of the quantitative effects of rescattering. It should also be noted that calculation of rescattering effects carries a very heavy penalty in CPU time consumption, since it is necessary to follow in detail the complete space-time history of all involved particles. Increases of one or two orders of magnitude in CPU time are typically observed when rescattering effects are included.

The present version of MARCO only keeps track of the

forward or backward momentum loss of a baryon. Another potential improvement can be implemented by providing a more detailed description of the internal excitation of the baryonlike object as it makes successive collisions.

V. CONCLUSIONS

We have performed a systematic comparison between the high energy nuclear collision Monte Carlo model MARCO and the WA80 calorimeter results concerning forward energy, transverse energy, and $dE_T/d\eta$ distributions. The comparison covers beam energies from 60A GeV to 200A GeV, projectiles of ^{16}O and ^{32}S and targets ranging from ^{12}C to ^{197}Au and pseudorapidities around midrapidity and forward.

Considering the simplicity of MARCO the general agreement between the model and data is remarkable. The

maximum values of the $dE_T/d\eta$ distributions are in most cases reproduced within $\approx 10\%$, the η position of the maximum is generally reproduced within 0.2 units of η and finally there is very close agreement between the calculated and measured widths.

ACKNOWLEDGMENTS

The authors wish to thank Dr. Sa Ben-Hao and Dr. Chao Wei-Qin for stimulating discussions. We appreciate the support of the Computing Center at the University of Tennessee, Knoxville, where all computations were done on the VAX9000 system. The research was supported by the Division of Nuclear Physics, U.S. Department of Energy (DOE) under Contract No. DE-AC05-84OR21400 with Martin Marietta Energy Systems, Inc. and the Department of Physics at University of Tennessee under DOE Contract No. DEAS05-76ER04936.

-
- [1] Proceedings, Quark Matter 90, Menton, France, 1990, Nucl. Phys. **A525** (1991).
 - [2] Proceedings, Quark Matter 91, Gatlinburg, TN, 1991 (to be published in Nucl. Phys. A).
 - [3] C.-Y. Wong and Z.-D. Lu, Phys. Rev. D **39**, 2606 (1989).
 - [4] WA80 Collaboration, R. Albrecht *et al.*, Phys. Rev. C **44**, 2736 (1991).
 - [5] K. Kinoshita, A. Minaka, and H. Sumiyoshi, Prog. Theor. Phys. **63**, 1268 (1980).
 - [6] K. Werner, Phys. Lett. B **208**, 520 (1988); Phys. Rev. Lett. **62**, 2460 (1989); Z. Phys. C **42**, 85 (1989); K. Werner and P. Koch, Phys. Lett. B **242**, 251 (1990).
 - [7] J. Ranft, Phys. Rev. D **37**, 1842 (1988); Z. Phys. C **43**, 439 (1989).
 - [8] T. Ludlam *et al.*, BNL Report No. 51921, 1985 (unpublished); A. Shor and S. Longacre, Phys. Lett. B **218**, 100 (1989).